

# Radial DLA: two fractal dimensions and deviations from linear self-similarity

Benoit B. Mandelbrot<sup>a</sup>, Boaz Kol<sup>b</sup> and Amnon Aharony<sup>b</sup>

<sup>a</sup>*Department of Mathematics, Yale University, New Haven, CT 06520-8283*

<sup>b</sup>*School of Physics and Astronomy, Raymond and Beverly Sackler Faculty of Exact Sciences,  
Tel Aviv University, Tel Aviv 69978, Israel*

(December 2, 2024)

When suitably rescaled, the distribution of the angular gaps between branches of off-lattice radial DLA is shown to approach a size-independent limit. The power-law expected from an asymptotic fractal dimension  $D = 1.71$  arises only for very small angular gaps, which occur only for clusters significantly larger than  $M = 10^6$  particles. Intermediate size gaps exhibit an effective dimension around 1.66, even for  $M \rightarrow \infty$ . They dominate the distribution for clusters with  $M < 10^6$ . The largest gap approaches a finite limit extremely slowly, with a correction of order  $M^{-0.17}$ .

PACS numbers: 61.43.Hv, 05.45.Df, 47.53.+n

For twenty years, a considerable effort has been devoted to the analysis of diffusion limited aggregation (DLA) [1], a model of many natural fractal growth processes. Even though DLA has no characteristic length scale, simulations exhibit nontrivial and ambiguous characteristics [2,3]. In the plane, the fractal dimension  $D = 1.71$  is usually associated with radial DLA [4], and  $D = 1.66$  is associated with cylindrical DLA [5–8].

Some measurements suggest that DLA has 5 main arms (or branches) [9]. In fact, larger clusters have more arms [10]. Figure 1 compares two DLA clusters, with  $M = 10^5$  and  $M = 10^8$  particles. One recognizes about 5 main arms for the  $M = 10^5$  cluster, but 8 or 9 arms in the  $M = 10^8$  cluster. This makes the  $M = 10^8$  cluster look more dense (like a filled circular disc), as argued in Refs. [2,3]. Different interpretations of the number of arms may, however, lead to contradictory results. Here we present a systematic way to describe this structural feature, based on the statistics of angular gaps between branches.

Our principal new finding is as follows: Scaling each gap by the sum of the 50 largest gaps yields a data collapse, which (in the absence of contrary evidence) we hypothesize characterizes the limit for  $M \rightarrow \infty$ . Intermediate size gaps exhibit an effective dimension around 1.66, and one needs very small gaps, hence very large clusters, to observe the correct asymptotic behavior with dimension  $D = 1.71$ . That is, the two widely quoted values of  $D$  are both present in radial DLA.

The intermediate dimension around 1.66 does not disappear as  $M \rightarrow \infty$ . Therefore, DLA cannot be modeled by any of the linearly self-similar fractals endowed with a unique fractal dimension. For many phenomena, like percolation, random “linear fractals” are good models and non-random linear fractals provide illuminating “cartoons”. This is a remarkable token of simplicity: after all, despite their diversity, linear fractals are counterparts of the Euclidean lines or planes. It is now clear that the sharp increase in complexity that occurs beyond linear self-similarity is inescapable for DLA and probably for

many other phenomena as well.

We also find that the typical largest gap (which gives some measure of the number of arms) approaches a *finite* limit, with an amazingly slow correction of order  $M^{-\gamma}$ , where  $\gamma = (2 - D)/D = 0.17$ . This slowly decaying correction may or may not be related to the slowly varying corrections recently found using a conformal map approach [11,12].

We performed very large scale simulations of off-lattice radial DLA, and focussed on the scaling properties of gaps on circular cross-cuts. An earlier analysis [3], based on clusters with up to  $10^7$  particles, yielded an apparent fractal dimension  $D = 1.65 \pm 0.01$ , which is not consistent with the widely accepted mass-radius dimension  $D = 1.71$ . Our software is as described in Ref. [13], but uses a single diffusing particle each time, as in the definition of DLA [1]. We generated  $N_c(M) = 1000$  clusters with  $M = 10^5, 10^{5.5}, 10^6, 10^{6.5}$  and  $10^7$  particles, plus  $N_c(M) = 60$  additional clusters with  $M = 10^{7.5}$  and  $10^8$  particles.

We endeavored to keep to the edge of the non-growing region. Trial and error [2,3] singled out particles whose distance  $R$  from the origin is within  $0.75R_g - 1 < R < 0.75R_g + 1$  (in units of the particle diameter), where  $R_g$  is the aggregate’s radius of gyration. Other radii were also considered, as mentioned at the end of this paper. The gap  $\theta$  is the difference in the polar angles between consecutive particle centers. To avoid “gaps” between touching particles, we keep only the values  $\theta > 1/0.75R_g$ , larger than one particle diameter. We then pool the gaps from all the available clusters of size  $M$  into a single list, which is sorted from largest to smallest. Thus each gap is characterized by its size and an integer  $r$  that represents its rank in the sorted list. Expecting  $r$  to grow linearly with  $N_c(M)$ , we use the mean-rank,  $\rho \equiv r/N_c(M)$ . For  $N_c \rightarrow \infty$ ,  $\rho$  becomes a continuous variable.

For an ideal linearly self-similar fractal of dimension  $D$ , one expects a power law,  $\theta \propto \rho^{-\alpha}$ , where  $\alpha \equiv 1/D_c$  and  $D_c \equiv D - 1$  is the fractal dimension of the intersection [14]. In contrast, Fig. 2 shows that  $\theta(\rho, M = 10^8)$ , based on the available  $N_c(10^8) = 60$  clusters, exhibits four dis-

tinct regions. Region I, which extends roughly for  $\rho < 10$ , reflects the statistics of the largest gaps. As in the Zipf-Mandelbrot distribution [14], the flattening of the curve in this region is a token of an upper cutoff (though not necessarily a sharp one) on the size of gaps. Both Regions II and III appear to be linear (see dashed lines in Fig. 2). In Region II, with  $10 < \rho < 50$ , the apparent slope is  $\alpha_{II} \cong 1.5$ , corresponding to  $D_{II} \cong 1.67$ . In estimating a slope, a broader range of  $\theta$  and  $\rho$  would have been better, but the validity of our estimate is strengthened by the fact that each of many separate simulations gave the same result. In Region III, with  $50 < \rho < \rho_{\max}/3$ , where  $\rho_{\max}(M = 10^8) = 1890$  is the maximal  $\rho$  for which  $\theta$  is defined (i.e. the average total number of gaps), the apparent slope is  $\alpha_{III} \cong 1.33$ , corresponding to  $D_{III} \cong 1.75$ . Region IV, with  $\rho_{\max}/3 < \rho < \rho_{\max}$ , reflects finite-size corrections: as  $M \rightarrow \infty$  one has  $\rho_{\max} \rightarrow \infty$ , and Region III extends to infinity, reflecting the asymptotic behavior of DLA. Since  $\rho_{\max}$  increases with  $M$ , it also follows that for  $M$  smaller than about  $10^6$ , Region III merges with Region IV, and one would mistakenly identify  $D$  from the higher apparent slope of Region II. This clearly demonstrates why one must have very large clusters to make statements about the asymptotic behavior of DLA.

A quantitative way to describe the crossover between Region II and III would involve corrections to the asymptotic power law. Since our data are not sufficient to determine these corrections, we represent the data by an ad-hoc parametric power expansion,

$$\theta(\rho) = \sum_{k=1}^{k_{\max}} a_k \rho^{-k\alpha} = \sum_{k=1}^{k_{\max}} a_k x^k, \quad (1)$$

where  $x = \rho^{-\alpha}$ . Using  $\alpha = 1.4$ , this form ensures the asymptotic dimension  $D = 1.71$  for large  $\rho$ . A least squares fit with  $k_{\max} = 6$  to the data for  $10 < \rho < \rho_{\max}/3 = 630$  at  $M = 10^8$  yields  $a_k = 3.702, -126.7, 1.566 \times 10^4, -8.045 \times 10^5, 1.901 \times 10^7, -1.694 \times 10^8$ . This yields an approximate effective dimension,  $D_{\text{eff}}(\rho) \equiv 1 + 1/\alpha_{\text{eff}}$ , where  $\alpha_{\text{eff}}(\rho) \equiv -d(\log \theta)/d(\log \rho) = \alpha \frac{x}{\theta} \frac{d\theta}{dx}$ . Figure 3 shows the resulting  $D_{\text{eff}}(\rho)$ . Indeed,  $D_{\text{eff}}$  reaches a minimum of about 1.66 close to  $\rho = 20$  (in Region II), and a maximum of about 1.74 around  $\rho = 80$  (in the beginning of Region III). It approaches the asymptotic  $D = 1.71$  at larger  $\rho$ .

We next demonstrate scaling and data collapse. We scale  $\theta$  as

$$\theta(\rho, M) = S(M)\theta_n(\rho), \quad (2)$$

with

$$S(M) \equiv \int_0^G \theta(\rho, M) d\rho, \quad (3)$$

representing the largest gaps.  $G$  should be large enough in order to filter more of the statistical variance, but not

too large as to include finite-size corrections. The results are not very sensitive to  $G$ . The choice  $G = 50$ , at the beginning of the asymptotic slope (Region III), gives good results and facilitates some of the theoretical analysis presented later. Figure 4 shows  $\theta_n(\rho)$  for the different values of  $M$ . Clearly, all the graphs collapse onto a universal curve, except for deviations at large  $\rho$  (Region IV), due to finite-size corrections.

The curves in Fig. 4 end at  $\rho_{\max}(M)$ . The figure clearly shows fixed distances between consecutive end-points, indicating power-law dependences of both  $\rho_{\max}$  and of  $\theta(\rho_{\max})$  on  $M$ . Since  $\rho_{\max}$  is the average number of gaps (or particles) on the annulus of radius  $R$ , we expect that  $\rho_{\max} \propto R^{D-1} \propto M^{(D-1)/D}$ . The smallest gap is then expected to scale as  $1/R \propto 1/M^{1/D}$ . We thus expect the small gaps to scale as

$$\theta(\rho, M) = M^{-1/D} f(\rho^{1/(D-1)}/M^{1/D}). \quad (4)$$

Indeed, Fig. 5 shows  $M^{1/D}\theta$  plotted vs.  $\rho^{1/(D-1)}/M^{1/D}$  for various  $M$ 's. There is a clear data collapse on the right-hand side, in agreement with Eq. (4).

We next use the collapse of the normalized gaps in Fig. 4 to infer about the asymptotic limit of the distribution of the original (non-normalized) gaps as a function of  $M$ . As expected, the collapse shows that apart from finite size corrections (i.e. for  $\rho < \rho_{\max}/3$ ),  $\theta_n$  depends only on  $\rho$ , and *not* on  $M$ . The  $M$ -dependence of the original gaps,  $\theta(\rho, M) = S(M)\theta_n(\rho)$ , is thus determined by the scale factor  $S(M)$ . Integrating over  $\rho$  on both sides of Eq. (2), the left hand side becomes  $\int_0^{\rho_{\max}} \theta(\rho, M) = 2\pi - X$ , equal to the average sum (over all cluster realizations) of all the gaps;  $X$  is the sum over the gaps that are smaller than one diameter. We expect that  $X \propto \rho_{\max}/R_g$ , and therefore  $X = B_1 M^{-\gamma}$ , with  $\gamma \equiv (2 - D)/D = 0.17$ . On the right hand side, we divide the integral into three parts:  $0 < \rho < G$ ,  $G < \rho < \rho_{\max}/3$  and  $\rho_{\max}/3 < \rho < \rho_{\max}$ . Equation (3) implies that  $\int_0^G \theta_n d\rho \equiv 1$ . The second integral belongs to Region III, where we write  $\theta_n(\rho) \simeq A_1 \rho^{-\alpha}$ , and  $A_1 = a_1/S(10^8) = 0.77 \pm 0.01$  is independent of  $M$  (as seen from Fig. 4). This yields  $B_2[G^{-\beta} - (\rho_{\max}/3)^{-\beta}]$ , with  $\beta = (2 - D)/(D - 1)$  and  $B_2 = A_1/\beta$ . Since  $\rho_{\max} \propto M^{(D-1)/D}$ , we conclude that the integral over the right hand side is equal to  $S(M)(A - B_3 M^{-\gamma})$ , where  $A = 1 + B_2 G^{-\beta} = 1.40 \pm 0.01$  and  $B_3$  is a constant (which is also affected by  $\int_{\rho_{\max}/3}^{\rho_{\max}} \theta_n d\rho \sim M^{-\gamma}$ , due to Eq. (4)). Our conclusion is that for large  $M$  one has

$$S(M) = \frac{2\pi - B_1 M^{-\gamma}}{A - B_3 M^{-\gamma}}, \quad (5)$$

and hence  $\theta(\rho, M = \infty) = (2\pi/A)\theta_n(\rho) \cong 4.5\theta_n(\rho)$ .

While the distribution of gaps does converge to a limit for  $M \rightarrow \infty$ , this convergence is *amazingly* slow, being governed by the small exponent  $\gamma$ : The correction term in Eq. (5) reduces only by a factor of  $10^{3 \times 0.17} \simeq 3.2$ ,

between  $M = 10^5$  and  $M = 10^8$ ! This means that great caution should be taken when extrapolating various measurements in DLA, and that the asymptotic limit (whose existence is generally expected) is attained only for extremely large  $M$ . Recently, Somfai *et al.* [11] also found a slow crossover to the asymptotic behavior of the squared characteristic lengths, with a correction exponent  $\phi = 0.3 \pm 0.1$ .

We next examine the statistics of the largest gaps,  $\{\theta_{\max}\}$ . For a linearly self-similar fractal, one expects to find the same distribution of the  $\{\theta_{\max}\}$ 's for different cluster sizes.  $\{\theta_{\max}\}$  may also relate to the number of main branches. For example,  $\{\theta_{\max}\} \approx 2\pi/5$  may indicate that the number of main branches is around 5. It has been shown that  $\{\theta_{\max}\}$  decays slowly with  $M$  [3], which means that the number of main branches increases, raising doubts on the self-similarity of DLA at intermediate values of  $M$ .

If, instead of pooling, we had studied the gaps of a single cluster, then we would have  $\{\theta_{\max}\} = \theta(r = 1)$ . However, the mean-rank  $\rho = 1$  has a different meaning:  $\theta(\rho = 1, M)$  is the  $N_c$ 'th largest gap out of all the gaps taken from  $N_c$  clusters. Since the graph of  $\theta_n(\rho, M)$  is relatively flat near  $\rho = 1$ , we still expect  $\theta(\rho = 1, M)$  to represent the order of magnitude of the average largest gap. Reading  $\theta_n(\rho = 1) = 0.1$  from the universal curve in Fig. 4, we estimate  $\theta(\rho = 1, M = \infty) = (2\pi/A)\theta_n(1) \cong 0.45$ , in radians, yielding an asymptotic average maximal gap around  $26^\circ$  and implying a finite number of arms.

An alternative way to estimate  $\{\theta_{\max}\}$  is based on a direct study of the distribution of the  $\{\theta_{\max}\}$ 's for different clusters with the same  $M$ . This histogram, shown in Fig. 6 for  $M = 10^7$ , is quite broad. A fit to a log-normal form (also shown) yields  $\mu = \langle \ln \theta_{\max} \rangle \cong -0.50$  and  $\sigma = \langle (\ln \theta_{\max} - \mu)^2 \rangle \cong 0.22$ . We find a very slow decrease of  $\mu$  with  $M$ , approaching a finite limiting value of the order of magnitude given above [15].

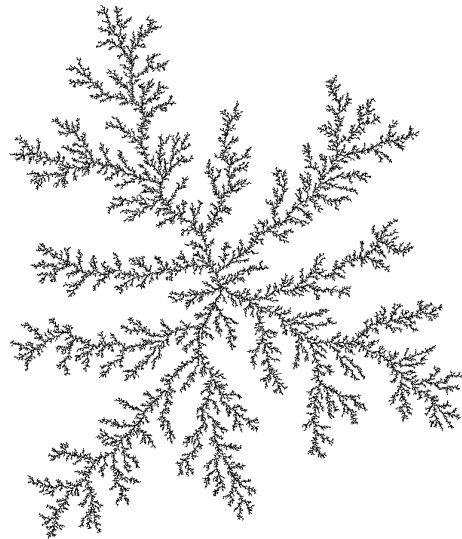
The broad distribution of  $\theta_{\max}$  implies that these largest pooled gaps spread over a broad range of  $\rho$ . This list convolutes the distributions of two non-independent quantities: the gaps for each cluster and the different clusters. For additional insight into these distributions, we also considered the correlations between gaps within each clusters. We find several interesting results: the average correlation between the largest gap and the  $r$ 'th gap for  $M = 10^7$  turns out to decrease from 1 to 0 (around  $r = 5$ ), and to approach a constant around  $-0.5$  for  $r > 10$  [15]. Such negative correlations are not surprising, since the total sum of the gaps must equal  $2\pi$ . The implications of these correlations on the pooled gap distribution remain for future study.

A brief additional study, with the collaboration of Eugene Vilensky of Yale, tested our results' sensitivity to the special choice of  $R \sim 0.75R_g$ . An increase of  $R$  beyond this value first leads to little change (confirming [2,3]), then to opposite changes in different regions: Very

large gaps come to dominate in Region I, moving the corresponding "flat" portion of the curve to higher values of  $\theta$ . The remaining gaps (other than the few largest) add to a decreasing total angle, but with little change in distribution.

Henry Kaufman kindly adapted his DLA program to serve our needs. This work has been supported in part by the German-Israeli Foundation (GIF).

- 
- [1] T. A. Witten and L. M. Sander, Phys. Rev. Lett. **47**, 1400 (1981); Phys. Rev. B **27**, 5686 (1983).
  - [2] B. B. Mandelbrot, H. Kaufman, A. Vespignani, I. Yekutieli, and C. H. Lam, Euro. Phys. Lett. **29**, 599 (1995).
  - [3] B. B. Mandelbrot, A. Vespignani, and H. Kaufman, Euro. Phys. Lett. **32**, 199 (1995).
  - [4] S. Tolman and P. Meakin, Phys. Rev. A **40**, 428 (1989).
  - [5] A. Erzan, L. Pietronero, and A. Vespignani, Rev. Mod. Phys. **67**, 545 (1995).
  - [6] P. Meakin and F. Family, Phys. Rev. A, **34**, 2558 (1986).
  - [7] B. Kol and A. Aharony, Phys. Rev. E **62**, 2531 (2000).
  - [8] B. Kol and A. Aharony, Phys. Rev. E **63**, 046117 (2001).
  - [9] A. Arneodo, F. Argoul, E. Bacry, J. F. Muzy, and M. Tabard, Phys. Rev. Lett. **68**, 3456 (1992).
  - [10] B. B. Mandelbrot, Physica A **191**, 95 (1992).
  - [11] E. Somfai, L. M. Sander, and R. C. Ball, Phys. Rev. Lett. **83**, 5523 (1999).
  - [12] B. Davidovitch and I. Procaccia, Phys. Rev. Lett. **85**, 3608 (2000).
  - [13] H. Kaufman, A. Vespignani, B. B. Mandelbrot and L. Woog, Phys. Rev. E **52**, 5602 (1995).
  - [14] B. B. Mandelbrot, *The Fractal Geometry of Nature* (Freeman, New York, 1982).
  - [15] B. Kol, Ph. D. thesis, Tel Aviv University, 2001.



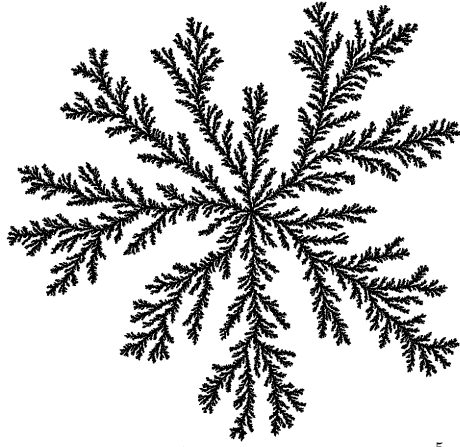


FIG. 1. Two radial DLA clusters, with  $M = 10^5$  (top) and  $M = 10^8$  (bottom) particles.

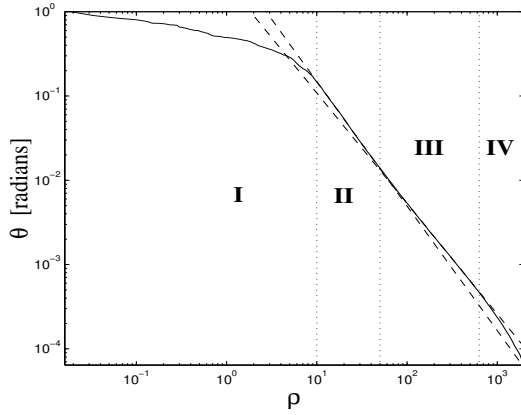


FIG. 2. The gap size  $\theta$  vs. the mean-rank  $\rho$ . The graph is based on 60 clusters with  $10^8$  particles. The dotted vertical lines separate the four regions discussed in the text. Dashed straight lines run through Regions II and III.

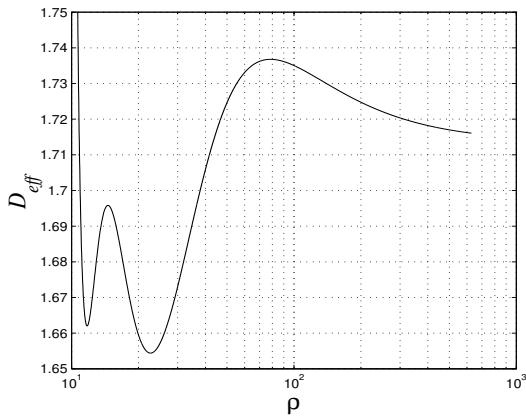


FIG. 3. Effective dimension  $D_{\text{eff}}(\rho)$ .

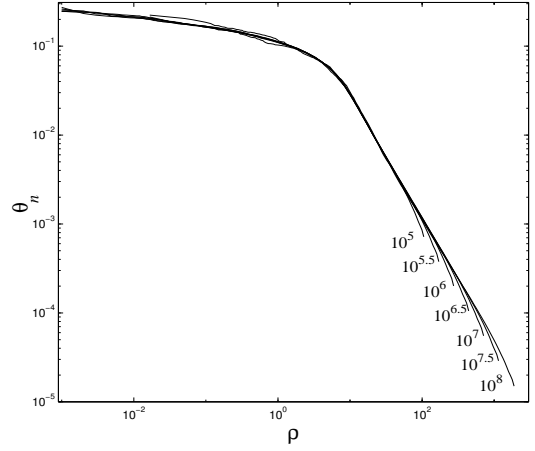


FIG. 4. Data collapse of  $\theta_n(\rho, M)$ . The numbers indicate the cluster size  $M$ .

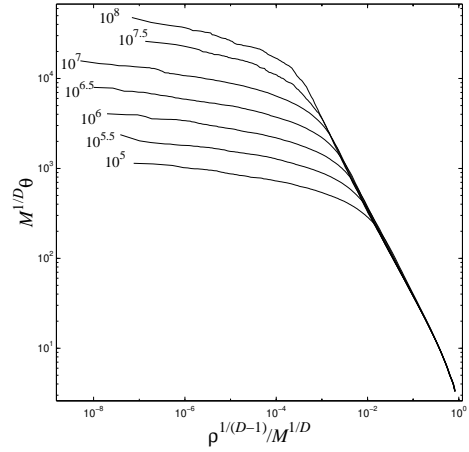


FIG. 5.  $M^{1/D}\theta$  vs.  $\rho^{1/(D-1)}/M^{1/D}$  for various values of  $M$ .

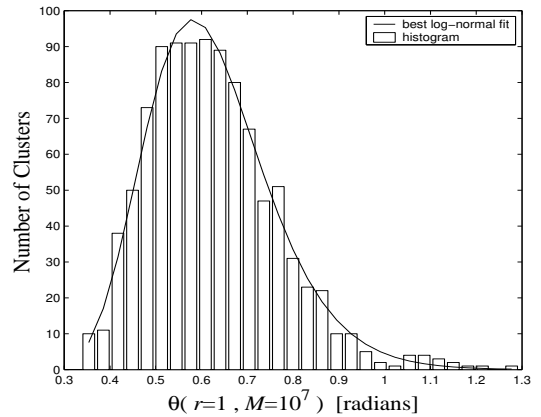


FIG. 6. Histogram of the maximal gap (in radians) in each cluster, for the 1000 available clusters with  $M = 10^7$ . The continuous line is the best fit to a log-normal distribution.